194

DYNAMICAL ENVIRONMENTS OF ORGANISED DEEP CONVECTION IN CLIMATE MODELS

Jackson Tan* and Christian Jakob
ARC Centre of Excellence for Climate System Science, Monash University, Melbourne, VIC, Australia

1 INTRODUCTION

A persistent shortcoming of all climate models is their inability to produce the correct distribution of precipitation, with light rain being too frequent and heavy precipitation being too rare (e.g. Sun et al. 2006, Stephens et al. 2010). In the tropics, intense rainfall is often associated with organised deep convection. Despite occurring only about 5% of the time, it contributes to about half the tropical precipitation (Tan et al., 2013) and is associated with extreme precipitation (Lee et al., 2013; Rossow et al., 2013).

Organised deep convection has a signature of extensive deep convective and thick stratiform anvil clouds. Such clouds are produced in global climate models (GCMs), but it is unclear if they are indeed the result of organised deep convection or products of some other processes. This stems from the fact that the organisation of convection is not explicitly taken into account in GCMs, in which convection is represented through parametrisation schemes. In these schemes, the statistical effects of convection are quantified through relationships with the resolved variables, but there is no explicit consideration of convective organisation, assuming instead that such organisation will emerge from the resolved variables. Hence, despite the existence of clouds which in observation is an indication of organised deep convection, it is unknown if models can replicate organised deep convection and its associated properties.

One way to identify organised deep convection in observation is through cloud regimes. First proposed by Jakob and Tselioudis (2003), these cloud regimes are derived from the statistical distributions of clouds within grids of resolution comparable to GCMs as measured by a network of satellites. As they are essentially categorisation of cloud fields in the atmosphere, the regime representing organised deep convection can easily be identified through its cloud profile. Indeed, Tan et al. (2013) have found that this regime is associated with conditions of organised deep convection such as intense precipitation and high grid-mean ascending motion.

By means of a satellite simulator, cloud regimes can also be defined in GCMs. Numerous studies have utilised cloud regimes in model evaluation and projections (Williams et al., 2005; Gordon et al., 2005; Williams and Tselioudis, 2007; Chen and Del Genio, 2008; Williams and Webb, 2008; Tsushima et al., 2012). However, they generally focus on the cloud profiles, geographical distributions and radiative properties of the model regimes. (Gordon et al. 2005 studied the large-scale properties such as relative humidity but for a single column model.) Here, we analyse the large-scale environment of the cloud regimes in GCM, similar to what Tan et al. (2013) have done in observation. In particular, we investigate the precipitation and vertical velocity distributions of the cloud regime that represents organised deep convection in observation, with the aims of examining whether this cloud regime is indicative of organised deep convection in models and hence if GCMs are capable of producing organised deep convection.

*Corresponding author address: Jackson Tan, School of Mathematical Sciences, Monash University, Clayton, VIC 3800, Australia. Email: Jackson.Tan@monash.edu

2 METHODS

2.1 Cloud Regimes

The International Satellite Cloud Climatology Project (ISCCP) D1 dataset provides statistical descriptions of clouds within 280 km $\times$ 280 km equal-area grids in the form of joint-histograms of their cloud top pressures and optical thickness since 1983 at three-hour intervals (Rossow and Schiffer, 1999). In the tropics, these joint-histograms are composed from satellite pixel measurements with an approximate horizontal resolution of 5 km at nadir from a network of geostationary satellites. Polar-orbiting satellites are used only when geostationary satellites are unavailable. In Jakob and Tselioudis (2003), the k-means clustering algorithm is applied to the joint-histograms to identify repeating patterns. In Rossow et al. (2005), this method is further improved upon by a set of criteria to determine the number of clusters. Applying this technique to daytime-averaged joint-histograms between 35° latitudes, cloud fields can be objectively categorized into eight cloud regimes (or weather states), of which three possess significant signals of deep convection (see Tan et al. 2013 for more information).

Of these three convective regimes, one describes an environment of organised deep convection. This regime, CR1 (called CD in Tan et al. 2013), has a prevalence of towering cumulus and deep stratiform clouds as interpreted in the joint-histogram of its centroid (Figure 1) and describes features such as thunderstorms and mesoscale

convective systems. It primarily inhabit regions of organised deep convection such as in the Intertropical Convergence Zone, the Tropical Western Pacific and Indian Oceans, and equatorial Africa and South America (Figure 2). Despite a low frequency of occurrence (FOC) of 0.055, it is associated with an exceptional levels of precipitation and is responsible for close to half the total precipitation in those latitudes (Lee et al., 2013; Tan et al., 2013). The other two convective regimes represent environments of less organised deep convection and are not the focus of this study.

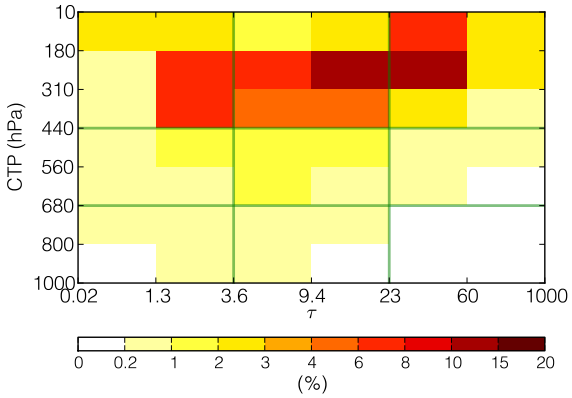

Figure 1: Joint-histogram of cloud top pressure (CTP) and optical thickness (τ) of the CR1 regime centroid in observation.

In global climate models (GCMs), such joint-histograms (variable: clisccp) can be derived for every grid box by means of the ISCCP satellite simulator, now part of the CFMIP (Cloud Feedback Model Intercomparison Project) Observation Simulator Package (Bodas-Salcedo et al., 2011). Hence, for GCMs participating in CFMIP under the CMIP5 framework (Coupled Model Intercomparison Project Phase 5), we are able to define cloud regimes. To do this, we use the method employed in Williams and Webb (2008), which follows that of Gordon et al. (2005) closely. Instead of assigning the joint-histograms to a regime based on its 42-dimensional vector (7 CTP bins $\times$ 6 τ bins), the joint-histograms are reduced to a three-dimensional vector comprising its mean albedo, mean cloud top pressure and total cloud cover, normalised to a range of 0 to 1. They are then assigned their regime membership by comparing them with the equivalent reduction of the centroids of *observed* regimes. If the model joint-histograms were to be assigned based on its full 42-dimensional vector, then a model that produces a cloud pixel incorrectly in a neighbouring CTP or τ bin is treated as equally as in any other erroneous bin. This alternative approach avoids such an unfair penalty and provides a greater degree of tolerance in the identification of model cloud regimes.

As the models output the joint-histograms with a daily time resolution, we shall use cloud regimes at daily resolution as well. This is obtained by working with daytime-averages of the ISCCP joint-histograms, prior to the clustering and assigning steps. This has the additional benefit of circumventing the issue of the unavailability of joint-histograms and hence cloud regimes at night. We restrict ourselves to ocean grid boxes, as the cloud regimes suffer from orographic artefacts (see Tan et al. 2013). We also constrain ourselves to five years of data from 2004 to 2008, which is sufficiently robust for our purposes. To simplify our analysis, we interpolate the observed cloud regime field to 2.5° $\times$ 2.5° grids using the nearest-neighbour technique.

2.2 Precipitation and Vertical Velocity

To identify the precipitation P and vertical velocity ω distributions of the CR1, we follow Tan et al. (2013) and composite them with additional datasets. For P, we use the Global Precipitation Climatology Project One-Degree Daily dataset (Huffman et al., 2001), and linearly interpolate to the 2.5° $\times$ 2.5° grids of the cloud regimes. For ω, we use the European Centre for Medium-Range Weather Forecasts (ECMWF) Interim Re-Analysis (ERA-Interim; Dee et al. 2011), and linearly interpolate from the native 1.5° grids to match that of the cloud regimes, as well as average them over the original six-hour time interval to one day. We select ω at pressure-heights of 200 hPa, 500 hPa and 850 hPa to approximately represent the top, middle and bottom of the troposphere.

For the models, the variables 'pr' and 'wap' provide the P and ω values respectively. We choose model runs from the CMIP5 database with the 'amip' experiment setup. Since we need runs that report the 'clisccp', 'pr' and 'wap' variables, there are six that fulfil this requirement: CanAM4, GFDL-CM3, HadGEM2-A, IPSL-CM5B-LR, MIROC5, and MPI-ESM-LR. More model runs may be available in other experiments such as 'historical', but this is beyond the scope of this study.

3 RESULTS

The cloud regime CR1 can be readily derived in the six models we are studying. However, this regime identification is based solely on the cloud profile produced in each model. In observation, the abundance of high-topped and optically thick clouds in CR1 is a signature of organised deep convection. Such an interpretation on the convective state of the atmosphere does not necessarily hold in the models. As a matter of fact, the goal of this study is to investigate whether CR1 is indeed organised deep convection in the models. Therefore, we should not assume that the properties we will investigate in the GCMs are those of model organised deep convection.

The first avenue to probe the nature of CR1 is to study its geographical distribution (Figure 2). As mentioned in the Section 2.1, CR1 in the real world occurs in areas of organised deep convection. In the six GCMs, the geographical distributions of CR1 roughly match these regions. However, all models overestimate its occurrence, as evident from the overall frequencies of occurrence, with

CanAM4, GFDL-CM3 and MIROC5 being the worst offenders. The other three models, on the other hand, have regional deficiencies. HadGEM2-A is producing insufficient CR1 in the Maritime Continent, while IPSL-CM5B-LR and MPI-ESM-LR have a lack of CR1 in the Intertropical Convergence Zone. However, Figure 2 do not permit us to diagnose the causes of the biases. We do not know if these errors are the result of a flawed cloud scheme, or incorrect large-scale conditions that drive cloud formation, or both.

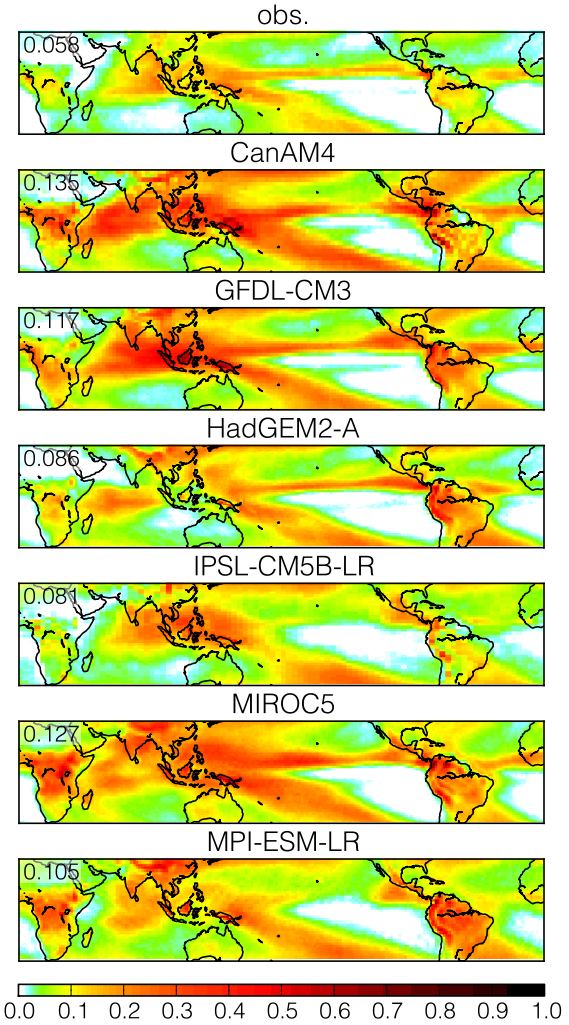

Figure 2: Geographical distributions of CR1 in observation and in models between 2004 to 2008. The numbers at the top-left indicate the overall frequencies of occurrence in the same period.

Figure 3 shows the distribution of the daily precipitation rates P associated with CR1 in observation and in models. Clearly but not surprisingly, most GCMs failed to achieve a mean P comparable to observation. Likewise, these GCMs do not match the observed P at high values ($P > 40$ mm / day). Only HadGEM2-A defies these two behaviours of GCMs and achieved a precipitation rate for CR1 that is similar to observation. However, all models, including HadGEM2-A, overestimate the incidence of light rainfall ($P < 5$ mm /day), which is a result, again, not surprising given the known tendency for GCMs to underpredict light rainfall and overpredict heavy rainfall.

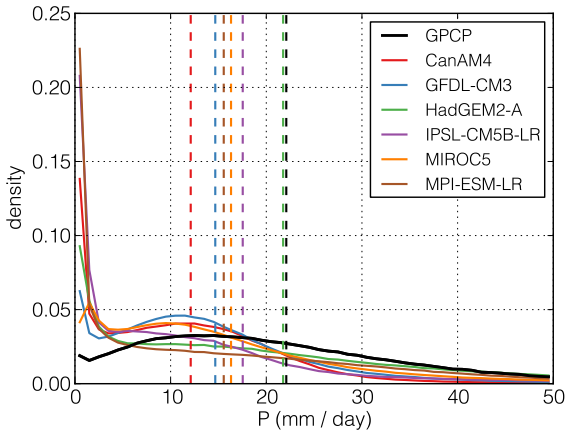

Figure 3: Distributions of daily precipitation rate P of CR1 in observation (GPCP) and models. The dashed vertical lines indicate the mean precipitation rates. Bin widths are 1 mm / day.

Notably, all models and observation have a jump in the first bin (0 mm / day $\leq P <$ 1 mm / day). Such incidences of low precipitation is uncommon in observation – hence the very small peak – but is severely overestimated in GCMs. This peak cannot be wholly attributable to the occurrences of CR1 with no precipitation ($P < 10^{-6}$ mm / day), as such occurrences only contribute to 10.2% of the counts in that bin in observation, 12.9% in IPSL-CM5B-LR, 28.8% in MPI-ESM-LR, and insignificant amounts in other models. In other words, GCMs are considerably overpredicting the occurrences of CR1 with precipitation that is very light but not zero. Curiously, the peak for MIROC5 occurs in the next bin, but the cause for this is unknown.

Figure 4 shows the distribution of grid-mean vertical motion ω at various heights associated with CR1 in observation and in models. At 200 hPa, all models overestimate the grid-mean ascending motion of CR1, i.e. producing values of ω_{200} that are too negative (Figure 4a). Furthermore, at more negative values of ω_{200}, e.g. $\omega_{200} = -0.3$ Pa / s, many models overestimate the incidence of such conditions by several times. This is also the case, albeit at a lesser degree, for strongly descending motion, e.g. $\omega_{200} > 0.1$ Pa / s. Essentially, many of the models produce a spread in ω_{200} of CR1 that is too large compared to reanalysis data.

At 500 hPa, some of these biases still exist but are less clear (Figure 4b). Most models overestimate the magnitude of mean ω_{500}, but CanAM4 now has a positive bias. Some models predict too frequent an occurrence of ω_{500} at the tail-ends, but not as excessive as at 200 hPa, primarily because such occurrences are more common in

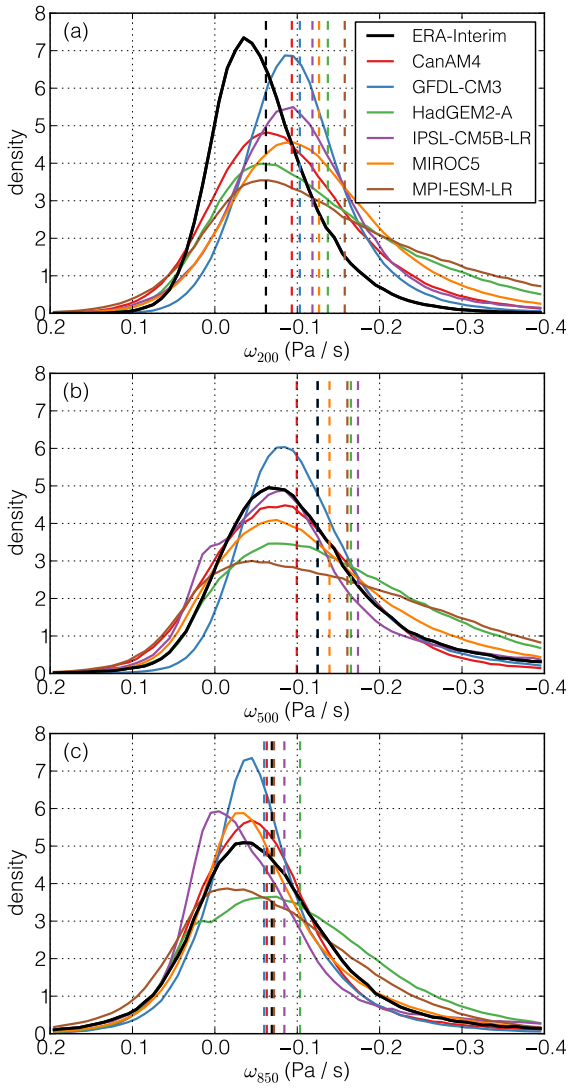

Figure 4: Distributions of grid-mean vertical motion ω at (a) 200 hPa, (b) 500 hPa, and (c) 850 hPa of CR1 in observation (ERA-Interim) and models. The dashed vertical lines indicate the mean ω. Bin widths are 0.01 Pa / s.

observation.

At 850 hPa, these biases become even more diluted (Figure 4c). The models do not collectively overestimate or underestimate the mean ω_{850}, and the range of the errors is narrower ($\sim$0.05 Pa / s for ω_{850} as opposed to $\sim$0.1 Pa / s for ω_{200}). In fact, many models perform reasonably well in predicting the ω_{850} of CR1.

Nevertheless, one qualitative observation that is apparent when comparing between Figure 3 and Figure 4 is the relationships between the biases in P and in ω. For example, HadGEM2-A has a distribution of P remarkably close to observation, but it consistently overestimates ω at all three levels, being one of the worst of all six models. On the other hand, CanAM4 is probably the best when judged based on its ω distribution, but its precipitation is plainly too low. This raises the question of whether there exist any relationship between the two errors, given that both variables are closely related to the deep convective process.

Figure 5 plots the biases in mean P against the biases in mean ω_{200}, mean ω_{500} and mean ω_{850} in a scatter diagram. It is clear that there is a relationship between these biases, with correlations that range from moderate (-0.54 at 200 hPa) to strong (-0.94 at 850 hPa). This means models that overestimate the grid-mean ascending motion of CR1 (too negative an ω) tend to produce precipitation rates that is closer to observation. It should be pointed out that ω in observation is obtained from ERA-Interim, which may possess biases itself as determining vertical motion remains a challenging task in numerical models. However, this should affect, to first order, the absolute values of observed ω (such as in Figure 4) and not the relative errors of the GCMs to observation (such as in Figure 5).

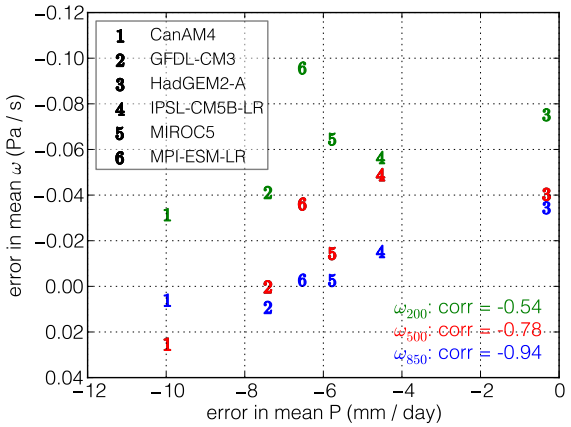

Figure 5: Scatter diagram of the errors (models $-$ observation) in mean P and mean ω at 200 hPa (green), 500 hPa (red) and 850 hPa (blue).

Naturally, one must be cautious in interpreting the correlations in Figure 5. To begin with, only six models are considered, which makes the correlation highly vulnerable to small changes in magnitudes of P or ω. In addition, the correlations do not capture the range in mean values between the models, which can be seen as an indication of how well the models represent this variable. For example, from Figure 4, one can infer that the models are better at predicting ω_{850} than ω_{200}, and yet the correlation is much higher for the former than the latter. Therefore, one should not place too much emphasis on the degree of correlation, and the main message of Figure 5 is to strengthen our previous observation that models tend to do less bad in P when they overestimate the magnitude of ω.

4 DISCUSSION AND CONCLUSION

In the previous section, we examined the properties of CR1 in models through its geographical distribution, daily

precipitation rates P and grid-mean vertical motion ω. The CR1 regime describes an environment with considerable amounts of high-topped and optically thick clouds, which in observation indicates organised deep convection. We found that models generally underestimate P and predicts a value of ω that is too negative, especially at 200 hPa. Furthermore, we discovered that these two errors are related, such that a model which overestimates the ascending motion tends to produce rainfall that is closer to observation.

The tendency for models to produce insufficient heavy rainfall and too much light precipitation is a well-known problem (Stephens et al., 2010). This issue, especially for heavy precipitation, is often linked to convective parametrisation schemes (Sun et al., 2006). Current schemes do not explicitly account for organisation (Yano et al., 2012), assuming instead that such organisation can manifest from the large-scale conditions that drive the schemes. Notwithstanding, the GCMs studied here still develop the high-topped and optically thick clouds of CR1, clouds which in observation are indications of organised deep convection. We conjecture that in order for GCMs to generate sufficient quantities of such clouds (and precipitation) to produce CR1, the convective parametrisation scheme exaggerates the area of deep convection, as evidenced by the excessive grid-mean ascending motion, so as to compensate for the lack of convective organisation.

If this conjecture is true, then it is imperative to account for the organisation of convection. Recent observational studies have found that different degrees of organisation may emerge from similar large-scale environments (e.g. Tobin et al. 2013, Tan et al. 2013), bringing into question the assumption that organisation can emerge from the resolved variables. Our conclusion is in line with the growing body of evidence that organised deep convection needs to be better represented in models, elevating the need for the development of schemes that explicitly account for organisation, such as Mapes and Neale (2011).

In conclusion, we studied the precipitation and vertical velocity distribution of a cloud regime with a high incidence of high-topped and optically thick clouds. In observation, this cloud regime characterise an environment of organised deep convection. In models, however, this cloud regime has too low a precipitation rate and too high a grid-mean ascending motion. On the basis that these two biases correlate, we conjecture that the convective parametrisation scheme overestimates the area of deep convection to make up for the absence of convective organisation. If so, this strengthens the need to account for convective organisation in global climate models.

Acknowledgements. This project is funded under the Australian Research Council Centre of Excellence for Climate System Science (grant number: CE110001028). We acknowledge Todd P. Lane and Steven Sherwood for their valuable comments, as well as Paola Petrelli from the Computational Modelling Systems team in the Centre of Excellence for her indispensable help on retrieving CMIP5 data.

References

Bodas-Salcedo, A., et al., 2011: COSP: Satellite simulation software for model assessment. *Bull. Amer. Meteor. Soc.*, **92**, 1023–1043, doi:10.1175/2011BAMS2856.1.

Chen, Y. and A. D. Del Genio, 2008: Evaluation of tropical cloud regimes in observations and a general circulation model. *Clim. Dynam.*, **32**, 355–369, doi:10.1007/s00382-008-0386-6.

Dee, D. P., et al., 2011: The ERA-Interim reanalysis: configuration and performance of the data assimilation system. *Quart. J. Roy. Meteor. Soc.*, **137**, 553–597, doi:10.1002/qj.828.

Gordon, N. D., J. R. Norris, C. P. Weaver, and S. A. Klein, 2005: Cluster analysis of cloud regimes and characteristic dynamics of midlatitude synoptic systems in observations and a model. *J. Geophys. Res.*, **110**, D15S17, doi:10.1029/2004JD005027.

Huffman, G. J., R. F. Adler, M. M. Morrissey, D. T. Bolvin, S. Curtis, R. Joyce, B. McGavock, and J. Susskind, 2001: Global Precipitation at One-Degree Daily Resolution from Multisatellite Observations. *J. Hydrometeor.*, **2**, 36–50, doi:10.1175/1525-7541(2001)002<0036:GPAODD>2.0.CO;2.

Jakob, C. and G. Tselioudis, 2003: Objective identification of cloud regimes in the Tropical Western Pacific. *Geophys. Res. Lett.*, **30**, 2082, doi:10.1029/2003GL018367.

Lee, D., L. Oreopoulos, G. J. Huffman, W. B. Rossow, and I.-S. Kang, 2013: The Precipitation Characteristics of ISCCP Tropical Weather States. *J. Climate*, **26**, 772–788, doi:10.1175/JCLI-D-11-00718.1.

Mapes, B. and R. Neale, 2011: Parameterizing Convective Organization to Escape the Entrainment Dilemma. *J. Adv. Model. Earth Sys.*, **3**, M06 004, doi:10.1029/2011MS000042.

Rossow, W. B., A. Mekonnen, C. Pearl, and W. Goncalves, 2013: Tropical Precipitation Extremes. *J. Climate*, **26**, 1457–1466, doi:10.1175/JCLI-D-11-00725.1.

Rossow, W. B. and R. A. Schiffer, 1999: Advances in Understanding Clouds from ISCCP. *Bull. Amer. Meteor. Soc.*, **80**, 2261–2287, doi:10.1175/1520-0477(1999)080<2261:AIUCFI>2.0.CO;2.

Rossow, W. B., G. Tselioudis, A. Polak, and C. Jakob, 2005: Tropical climate described as a distribution of weather states indicated by distinct mesoscale cloud property mixtures. *Geophys. Res. Lett.*, **32**, L21 812, doi:10.1029/2005GL024584.

Stephens, G. L., et al., 2010: Dreary state of precipitation in global models. *J. Geophys. Res.*, **115**, D24 211, doi:10.1029/2010JD014532.

Sun, Y., S. Solomon, A. Dai, and R. W. Portmann, 2006: How Often Does It Rain? *J. Climate*, **19**, 916–934, doi:10.1175/JCLI3672.1.

Tan, J., C. Jakob, and T. P. Lane, 2013: On the Identification of the Large-Scale Properties of Tropical Convection Using Cloud Regimes. *J. Climate*, **26**, 6618–6632, doi:10.1175/JCLI-D-12-00624.1.

Tobin, I., S. Bony, C. E. Holloway, J.-Y. Grandpeix, G. Sèze, D. Coppin, S. J. Woolnough, and R. Roca,

2013: Does convective aggregation need to be represented in cumulus parameterizations? *J. Adv. Model. Earth Sys.*, **5**, n/a–n/a, doi:10.1002/jame.20047.

Tsushima, Y., M. A. Ringer, M. J. Webb, and K. D. Williams, 2012: Quantitative evaluation of the seasonal variations in climate model cloud regimes. *Clim. Dynam.*, **41**, 2679–2696, doi:10.1007/s00382-012-1609-4.

Williams, K. D., C. a. Senior, A. Slingo, and J. F. B. Mitchell, 2005: Towards evaluating cloud response to climate change using clustering technique identification of cloud regimes. *Clim. Dynam.*, **24**, 701–719, doi:10.1007/s00382-004-0512-z.

Williams, K. D. and G. Tselioudis, 2007: GCM intercomparison of global cloud regimes: present-day evaluation and climate change response. *Clim. Dynam.*, **29**, 231–250, doi:10.1007/s00382-007-0232-2.

Williams, K. D. and M. J. Webb, 2008: A quantitative performance assessment of cloud regimes in climate models. *Clim. Dynam.*, **33**, 141–157, doi:10.1007/s00382-008-0443-1.

Yano, J.-I., H.-F. Graf, and F. Spineanu, 2012: Theoretical and Operational Implications of Atmospheric Convective Organization. *Bull. Amer. Meteor. Soc.*, **93**, ES39–ES41, doi:10.1175/BAMS-D-11-00178.1.